Approximation of super-ions for single-file diffusion of multiple ions through narrow pores

Valery N. Kharkyanen, Semen O. Yesylevskyy, and Natalia M. Berezetskaya
Department of Physics of Biological Systems, Institute of Physics, National Academy of Sciences of Ukraine, Prospect Nauki, 46, Kiev 03039, Ukraine

(Received 1 December 2009; revised manuscript received 19 September 2010; published 3 November 2010)

The general theory of the single-file multiparticle diffusion in the narrow pores could be greatly simplified in the case of inverted bell-like shape of the single-particle energy profile, which is often observed in biological ion channels. There is a narrow and deep groove in the energy landscape of multiple interacting ions in such profiles, which corresponds to the pre-defined optimal conduction pathway in the configurational space. If such groove exists, the motion of multiple ions can be reduced to the motion of single quasiparticle, called the superion, which moves in one-dimensional effective potential. The concept of the superions dramatically reduces the computational complexity of the problem and provides very clear physical interpretation of conduction phenomena in the narrow pores.

DOI: 10.1103/PhysRevE.82.051103 PACS number(s): 05.20.−y, 05.60.Cd, 87.10.Ca

I. INTRODUCTION

The narrow nanopores, which conduct ions or small molecules are widely known for their unique properties, which are not observed in macroscopic pores or bulk liquids. The particles in very narrow pores move in the single-file manner, while the number of particles changes stochastically due to exchange with surrounding solutions. The examples of such pores, which are very important for practical applications, are the ion channels of biological membranes [1–3] and the carbon nanotubes [4–6].

Narrow nanopores are studied extensively by means of molecular dynamics (MD) [7–9] or Brownian dynamics (BD) [8,10,11] simulations. This approach was very effective in revealing fine details of the conduction process and provided insight into the functioning of such practically important nanopores as the biological ion channels [8,11,12]. However, dedicated analytical theory of multi-ion diffusion in the narrow pores is often desirable in addition to these computational experiments. Such theory is independent on atomistic design of particular object and describes universal principles of diffusion in the narrow pores of any origin regardless of their atomistic details. It provides conceptual overview of possible phenomena in the pores, which may or may not be observed in particular system in particular conditions. The theory allows studying very wide range of pore parameters and external conditions. Finally, the theory could be used as an "ideal reference" for simulations or experimental studies.

Until recently no such theory was available. In our previous work we presented a theory, which fills this gap [13]. This theory is very general and describes the single-file diffusion of multiple ions in the narrow pores in nonequilibrium conditions. The ions move in arbitrary energy profile, created by the pore walls and the external electrostatic potential and interact explicitly by means or arbitrary repulsive potential. Any macroscopic property of the pore (such as a current or a mean occupancy) could be computed providing that these potentials and the concentrations of particles in surrounding solutions are known. It was shown that the problem is reduced to finding n-particle distribution functions inside the pore $\phi^{(n)}(x_1,\ldots,x_n;t)$ for all possible occupancies $M \geq n \geq 1$, where M is the maximal number of particles, which the pore can accommodate, x_i are the coordinates of the ions.

The problem of finding $\phi^{(n)}(x_1,\ldots,x_n;t)$ is independent from general analytical derivations and should be solved numerically for each particular system. Quite general way of finding $\phi^{(n)}(x_1,\ldots,x_n;t)$ was proposed in [13]. The distribution functions $\phi^{(n)}(x_1,\ldots,x_n;t)$ could be found from the closed hierarchical set of the Fokker-Plank equations of increasing dimensionality, which constitutes significant challenge in terms of the algorithms, convergence and precision [13]. We managed to solve some of these problems by providing generic computational procedure, which is applicable for arbitrary single-ion energy profile in the pore. Despite its generality this procedure remains rather intensive computationally and provides semiquantitative results as discussed in the "Results" section below.

In the present work we show that the general analytical theory developed in [13] can be greatly simplified in the case of specific inverted bell-like shape of the single-ion energy profile. The interest in such profiles is supported by their appearance in real ion channels [9,13,14]. The goal of this work is to study general physical principles of multiparticle diffusion in the potential of this class. We show that the multidimensional distribution functions of the ions inside the pore could be reduced to one-dimensional distribution functions of the quasiparticles (called the super-ions) in such potentials. All observed macroscopic properties of the pore are then described in terms of the super-ions. This approximation provides very simple and elegant description of the pore conductance. It also leads to very simple and effective numerical procedure of finding $\phi^{(n)}(x_1,\ldots,x_n;t)$, which is more precise then the generic computational procedure from [13] (providing that the approximation of the super-ions is valid for given energy profile).

The idea of the super-ions was already exploited (although in rather naïve manner) in our previous work [15]. This work provides much more formal and consistent definition of the super-ions, which is based on strict general theory developed in [13].

We use the results of the general theory developed in [13] in this work extensively, but do not repeat any derivations.

The reader is referred to [13] for detailed derivations and discussion.

II. THEORY

A. Boundary conditions

One of the problems, which arise in the analytical theories of the multiparticle diffusion, is the choice of the boundary conditions. The boundary conditions depend on the model of the pore boundary and the details of particle exchange events adopted in the theory. It is obvious that the particle, which leaves the pore, can reenter it with certain probability, which decreases with time and depends on the diffusion coefficient and the properties of the transition region between the pore and the bulk solution (the channel vestibule). As a consequence effective concentration of particles in the vicinity of the channel entrance differs from the concentration in the bulk solution [16]. The microscopic kinetic balance at the pore boundary is usually considered in order to describe complex events of particle escape and re-entrance. This method is the most straightforward, but it leads to complex boundary conditions, which contain unknown kinetic constants. The complexity of such boundary conditions is shown in details in the work of Stephan *et al.* [17], where the microscopic rate constant theory for the channel with multiple occupancy was developed systematically and transformed to the system of the Fokker-Planck equations in continuous limit [17]. The equations for n and n+1 particles are coupled by means of unknown kinetic parameters on the channel boundaries. The boundary conditions are quite nontrivial already in the case of two particles and become extremely complex in the general case. As a result the pores with more then two ions are not considered [17]. Another example of complex boundary conditions, which contain the current through the channel as a parameter, can be found in the work [16].

In the present work we follow an approach introduced in our general theory [13]. In this approach an explicit microscopic description of the ion exchange events is avoided, which greatly simplifies boundary conditions and distinguish our framework from existing analytical theories of the multiparticle diffusion.

It is assumed that the particle, which crosses the pore boundary and escapes to the solution, loses all correlations with the particles, which remain in the pore abruptly. This assumption is the key point of our theory. It means that the probability of reentry of the escaped particle is the same as the probability of entry of any other particle from the solution (the particle has no memory). As a result the solutions do not "feel" the presence of the pore and could be considered as ideal heat bathes with given concentrations of particles. This basic assumption can be either postulated or derived from dynamic equations in certain conditions as it is shown in Appendix B in [13]. It leads to convenient factorization of the probability density function at the channel boundary, which allows describing the events of entry and exit of the ions by the following simple boundary condition:

$$\phi^{(n)}(x_1,\ldots,x_n;t)_{x_i=\mp L} = c_{1,2}\phi^{(n-1)}(x_1,\ldots x_{i-1},x_{i+1}\ldots x_{n-1};t), \tag{1}$$

where $c_{1,2}$ are the concentrations of the ions in solutions, L is the half-length of the channel.

It is necessary to emphasize that Eq. (1) describes the exchange events between the pore and the solutions in a consistent way without any additional assumptions and kinetic parameters. It also couples otherwise independent distribution functions for different occupancy states into the hierarchy.

Equation (1) implies that there are no energy barriers between the channel and the solutions, so the exchange of particles between the channel and the reservoirs is purely diffusive. This does not limit the generality of our approach since any barriers, which may exist at the ends of particular channel, could be included into the channel itself and reflected by its single-ion energy profile. Further details and derivations could be found in [13].

B. Energy landscape of the pore

Simplified reference model of the pore with inverted bell-like single-ion energy profile is used in this work. This model was studied extensively in our previous works [13,15,18], which make it ideal for testing our concept of the super-ions. The interaction forces in this model are balanced in such a way that the ions are located at some "optimal" distance from each other most of the time and move in a highly concerted manner. Let us formalize this picture. The energy of n ions, which reside in the pore, is

$$U_n(\vec{x}) = \sum_{i=1}^{n} U_0(x_i) + \sum_{\substack{i,j=1 \\ (i>j)}}^{n} V(x_i - x_j), \tag{2}$$

where U_0 is the single-ion energy profile; V is repulsive ion-ion interaction potential; x_i is the coordinate of ith ion measured along the pore axis; $\vec{x}=\{x_1,x_2,\ldots,x_n\}$. $-L<x_i<L$, where L is the half-length of the pore. Single-file motion of the ions allows us to consider only a part of the whole configurational space where the ions are ordered from left to right $G^{(n)}=\{-L\le x_1\le x_2\le\ldots\le x_{n-1}\le x_n\le L\}$.

The single-ion energy profile U_0 has inverted bell-like shape, which could be described by the inverted Gaussian curve

$$U_0(x) = -A\,\exp(-x^2/s^2) + \psi\frac{x}{L}, \tag{3}$$

where A is the depth of the single-ion energy profile; s is the half-width of this profile. The second term describes the transmembrane electrostatic potential in the linear approximation (see Discussion in [13] for the rationale).

The ion-ion electrostatic interactions in our model are approximated by the shielded Coulomb potential

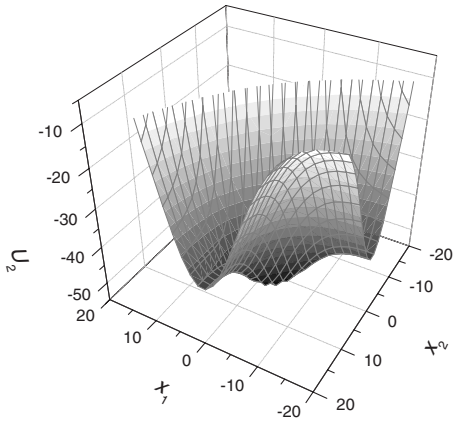

FIG. 1. The surface plot of U_2 for $A=40$ k_BT, $d=5$ Å. The groove is clearly visible.

$$V(r) = \frac{b}{r}\exp\left(-\frac{r}{d}\right), \tag{4}$$

where d is the shielding constant; b is the constant, which converts the electrostatic energy to the k_BT units. This interaction should be considered as the simplest reasonable approximation of the real ion-ion interaction inside the pore. The empirical constant d allows us to vary the amount of screening.

The values of empirical constants are $b=566.2$, $s=9$ Å, $L=20$ Å [15,18]. Free parameters A and d are varied. The configurations up to $M=4$ were considered to cover the whole range of possible pore occupancies. Detailed discussion of the various aspects of the reference model of the pore could be found in [15,18].

It is easy to deduce that concerted motion of the ions corresponds to some predefined "optimal" trajectory in n-dimensional configurational space. A bundle of trajectories in the close vicinity of this optimal path are sampled with high probability, while the probabilities of all other trajectories are negligible. Selected region of configurational space, where the most probable trajectories are located, obviously corresponds to a deep and rather narrow "groove" in U_n. Figures 1, 2(b), and 2(c) show the examples of such grooves in the cases $n=2,3$. If the groove is deep enough, then the probability density $\phi^{(n)}(x_1,\ldots,x_n,t)$ is negligible outside the groove, which simplifies the problem dramatically.

Let us define the groove axis, which corresponds to the bottom of the groove. The groove axis connects the points $M_1=\{-L,x_2',\ldots,x_n'\}$ and $M_2=\{x_1'',\ldots,x_{n-1}'',L\}$ located at the "input" and "output" facets of $G^{(n)}$, which correspond to x_1

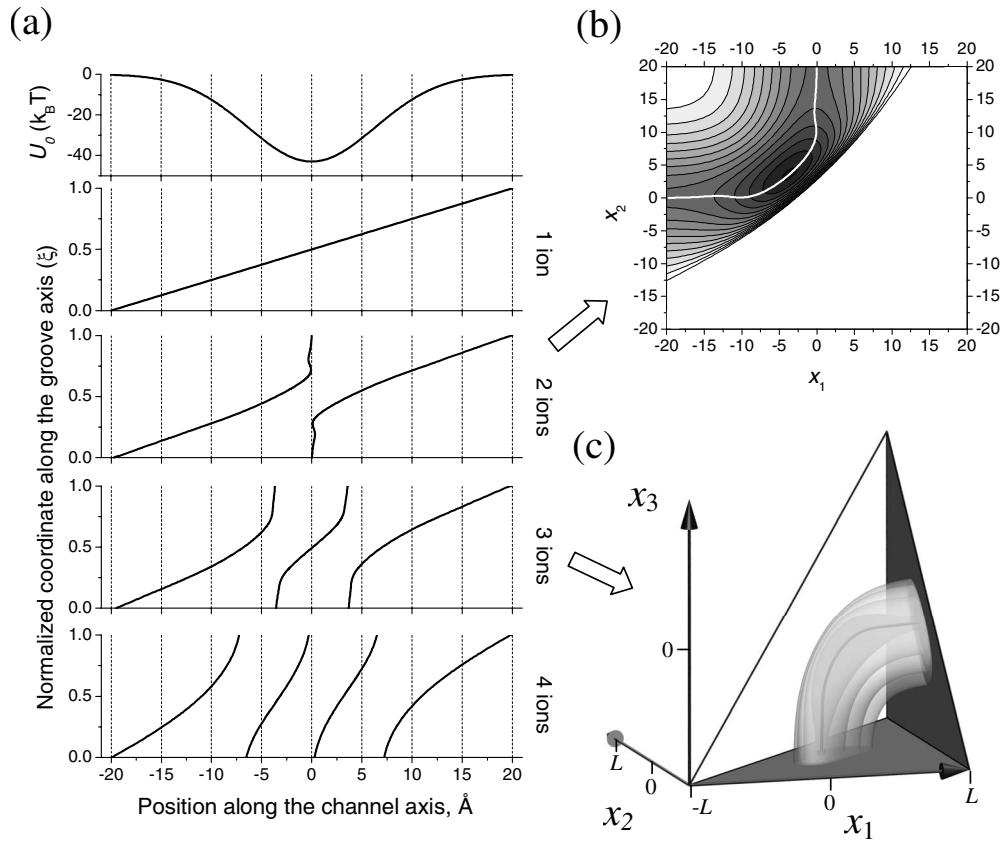

FIG. 2. The groove axis in various occupancy states for $A=43$ k_BT, $d=3$ Å. (a) The parametric coordinates of the groove axis for $n=1,\ldots,4$. ith curve in each particular panel (counting from the left) corresponds to the coordinate $x_i(\xi)$ of the groove axis. The coordinate ξ is normalized for clarity. Top panel shows the single-ion energy profile for the reference. (b) The contour plot of the potential U_2 (two ions in the channel) with the groove axis superimposed as a white line. (c) The plot of the isosurfaces of the three-dimensional potential U_3 (three ions in the channel). The isosurfaces are drawn at -66 k_BT, -60 k_BT, -54 k_BT, and -50 k_BT counting from inside out. The groove axis is shown as a solid line inside the isosurfaces.

$=-L$ and $x_n=L$, respectively. M_1 and M_2 are defined as $\frac{\partial U_n(-L,x_2,..,x_n)}{\partial x_i}=0$, $i=2,..,n$ and $\frac{\partial U_n(x_1,..,x_{n-1},L)}{\partial x_i}=0$, $i=1,..,n-1$ correspondingly. The axis could be parameterized by the length of the curve ξ_1 measured from M_1 toward M_2 as

$$\frac{d\vec{r}(\xi_1)}{d\xi_1}=\vec{\tau}^{(1)}(\xi_1), \tag{5}$$

where $\vec{r}(\xi_1)=\Sigma_{i=1}^{n}x_i^{(r)}(\xi_1)\vec{e}^{(i)}$ is the radius-vector of particular axis point, $x_i^{(r)}(\xi_1)$ are Cartesian coordinates of this point, $\vec{e}^{(i)}$ are the orts of the laboratory coordinate system,

$$\vec{\tau}^{(1)}=\frac{\sum_{i=1}^{n}\left|\frac{\partial U_n(\vec{x})}{\partial x_i}\right|\vec{e}_i}{\sqrt{\sum_{i=1}^{n}\left(\frac{\partial U_n(\vec{x})}{\partial x_i}\right)^2}} \tag{6}$$

is a vector tangential to the groove axis.

It is convenient to describe the motion inside the groove in its own local coordinate system, which defines the directions parallel and perpendicular to the groove axis. The parallel direction is given by $\vec{\tau}^{(1)}$, while remaining $n-1$ perpendicular directions lie in the hyperplane $\mathbb{N}(\xi_1)$, which is normal to $\vec{\tau}$ in particular point ξ_1 of the groove axis. $\mathbb{N}(\xi_1)$ is defined as

$$[R(\vec{x})-\vec{r}(\xi_1),\vec{\tau}^{(1)}(\xi_1)]=0, \tag{7}$$

where $R(\vec{x})$ is arbitrary point, which belongs to this hyperplane. Equation (7) could be rewritten as

$$\sum_{i=1}^{n}[x_i-x_i^{(r)}(\xi_1)]\left|\frac{\partial U_n(\vec{x})}{\partial x_i}\right|=0. \tag{8}$$

Let us define the system of $n-1$ orthonormal vectors in $\mathbb{N}(\xi_1)$

$$\vec{\tau}^{(\alpha)}(\xi_1)=\sum_{i=1}^{n}\tau_i^{(\alpha)}(\xi_1)\vec{e}^{(i)}, \tag{9}$$

where $\alpha=2,..,n$. Equations (9) and (6) define full orthonormal local coordinate system at each point of the groove axis. This system is valid in some small vicinity of the groove axis, which ensures that the hyperplanes $\mathbb{N}(\xi_1)$ and $\mathbb{N}(\xi_2)$ of any two points do not intersect. The correspondence between the points $\vec{x}$ and $\vec{x}^{(r)}$ in the laboratory and the local coordinate systems is given by

$$x_i(\vec{\xi})=x_i^{(r)}(\xi_1)+\sum_{\alpha=2}^{n}\xi_\alpha\tau_i^{(\alpha)}(\xi_1).$$

The potential [Eq. (2)] could be rewritten using local coordinates $\vec{\xi}\equiv\{\xi_\alpha\}$, $\alpha=1,..,n$ as

$$\tilde{U}_n(\vec{\xi})\equiv U_n\left[\vec{r}(\xi_1)+\sum_{\alpha=2}^{n}\xi_\alpha\vec{\tau}^{(\alpha)}(\xi_1)\right]. \tag{10}$$

The criterion of existence of the groove can be formalized easily as

$$\left.\frac{\partial\tilde{U}_n(\vec{\xi})}{\partial\xi_\alpha}\right|_{\xi_\alpha=0}=0,$$

$$\left|\frac{\partial\tilde{U}_n(\vec{\xi})}{\partial\xi_1}\right|\Bigg|_{\xi_\alpha=0}\ll\left|\frac{\partial^2\tilde{U}_n(\vec{\xi})}{\partial\xi_\alpha^2}\Delta_\alpha(\xi_1)\right|\Bigg|_{\xi_\alpha=0},$$

$$\alpha=2,..,n. \tag{11}$$

where $\alpha=2,..,n$; $\Delta_\alpha(\xi_1)$ is a characteristic half width of the groove in direction ξ_α in the point ξ_1. In the other words, the "side walls" of the groove are very steep in comparison with the profile of the groove bottom. It is also implied implicitly that the groove is deep enough.

C. Super-ions

As it was already mentioned in introduction, the general theory of the multiparticle diffusion in the narrow pore developed in [13] leads to a system of the multidimensional Fokker-Plank equations

$$\frac{\partial\phi^{(n)}(x_1,\ldots,x_n,t)}{\partial t}=D\sum_{i=1}^{n}\frac{\partial}{\partial x_i}\left[\frac{\partial U_n(x_1,\ldots,x_n)}{\partial x_i}\phi^{(n)}(\vec{x},t)+\frac{\partial\phi^{(n)}(x_1,\ldots,x_n,t)}{\partial x_i}\right], \tag{12}$$

where $\phi^{(n)}(x_1,\ldots,x_n,t)$ is the probability density in the case of exactly n ions in the pore, D is the diffusion coefficient. Equations (12) are subject to the boundary conditions [Eq. (1)], which form the hierarchical sequence of equations of the growing dimensionality.

The local coordinate system $\{\xi_i\}$ is curvilinear, but their Lame coefficients are all equal to 1

$$H_\alpha=\sqrt{\sum_{i=1}^{n}\left(\frac{\partial x_i}{\partial\xi_\alpha}\right)^2}=\sqrt{\sum_{i=1}^{n}[\tau_i^{(\alpha)}(\xi_1)]^2}=1.$$

This makes rewriting Eq. (12) in terms of $\{\xi_i\}$ trivial

$$\frac{\partial\tilde{\phi}^{(n)}(\vec{\xi};t)}{\partial t}=D\left\{\frac{\partial}{\partial\xi_1}\left[\frac{\partial\tilde{U}_n(\vec{\xi})}{\partial\xi_1}\tilde{\phi}^{(n)}(\vec{\xi};t)+\frac{\partial\tilde{\phi}^{(n)}(\vec{\xi};t)}{\partial\xi_1}\right]+\sum_{\alpha=2}^{n}\frac{\partial}{\partial\xi_\alpha}\left[\frac{\partial\tilde{U}_n(\vec{\xi})}{\partial\xi_\alpha}\tilde{\phi}^{(n)}(\vec{\xi};t)+\frac{\partial\tilde{\phi}^{(n)}(\vec{\xi};t)}{\partial\xi_\alpha}\right]\right\}, \tag{13}$$

where

$$\tilde{\phi}^{(n)}(\vec{\xi};t)=\phi^{(n)}\left[\vec{r}(\xi_1)+\sum_{\alpha=2}^{n}\xi_\alpha\vec{\tau}^{(\alpha)}(\xi_1);t\right]. \tag{14}$$

The first term of Eq. (13) describes rather slow relaxation along the groove (the potential is smooth and changes slowly along this direction). The second term describes very fast relaxation in the perpendicular cross section of the groove [the potential is extremely fast growing in this direction according to Eq. (11)]. As a result there are two phases of

relaxation of the function $\tilde{\phi}^{(n)}$ with very different characteristic times. We are only interested in the slow phase, which eventually leads to the steady-state flux along the groove, which determines all macroscopic characteristics of the pore. Therefore we can consider the system in the adiabatic approximation. At the times larger than the characteristic relaxation time in the perpendicular cross section of the groove the distribution function $\tilde{\phi}^{(n)}$ is in local equilibrium in any hyperplane $\mathbb{N}(\xi_1)$. As a result the solution of Eq. (13) can be written as

$$\tilde{\phi}^{(n)}(t;\vec{\xi}) = \varphi^{(n)}(t;\xi_1)\frac{e^{-\tilde{U}_n(\vec{\xi})}}{z_n(\xi_1)}, \tag{15}$$

where

$$z_n(\xi_1) = \int_{-\Delta_2}^{\Delta_2} d\xi_2, \ldots, \int_{-\Delta_n}^{\Delta_n} d\xi_n e^{-\tilde{U}_n(\vec{\xi})}. \tag{16}$$

The limits of integration Δ_i are chosen to ensure that $z_n(\xi_1)$ is independent on Δ_i. It is obvious that approximation [Eq. (15)] approaches exact solution with the increase of depth and the decrease of width of the groove.

Substitution of Eq. (15) into Eq. (13) and integration over the same variable and in the same limits as in Eq. (16) yields

$$\frac{\partial \varphi^{(n)}(t;\xi_1)}{\partial t} = D\frac{\partial}{\partial \xi_1}\left[\frac{\partial U_n^{eff}(\xi_1)}{\partial \xi_1}\varphi^{(n)}(t;\xi_1) + \frac{\partial \varphi^{(n)}(t;\xi_1)}{\partial \xi_1}\right], \tag{17}$$

where

$$U_n^{eff}(\xi_1) = \int_{-\Delta_2}^{\Delta_2} d\xi_2, \ldots, \int_{-\Delta_n}^{\Delta_n} d\xi_n \frac{\partial \tilde{U}_n(\vec{\xi})}{\partial \xi_1}\frac{e^{-\tilde{U}_n(\vec{\xi})}}{z_n(\xi_1)} = -\ln z_n(\xi_1) \tag{18}$$

is a local free energy in each hyperplane $\mathbb{N}(\xi_1)$ called an effective potential.

Equation (17) is essentially a one-dimensional Fokker-Plank equation for some collective quasiparticle, which moves along the groove axis in the effective potential [Eq. (18)]. We will call this quasiparticle a *super-ion* hereafter. It is necessary to emphasize that the super-ion moves along the curved one-dimensional groove axis in n-dimensional configurational space, while the real ions move along the pore axis in real space.

Approximated steady-state solution of Eq. (13) can be written in terms of the super-ions as

$$\tilde{\phi}^{(n)}(\vec{\xi}) = \begin{cases} \varphi^{(n)}(\xi_1)\dfrac{e^{-\tilde{U}_n(\vec{\xi})}}{z_n(\xi_1)}, & \vec{\xi} \in \mathfrak{R}^{(n)} \\ 0, & \vec{\xi} \notin \mathfrak{R}^{(n)} \end{cases}, \tag{19}$$

where $\mathfrak{R}^{(n)}$ is the part of the configurational space inside the groove [determined by the integration limits Δ_i in Eq. (16)]; $\varphi^{(n)}(\xi_1)$ is the steady-state solution of Eq. (17). This approximation is very close to exact solution if the groove is deep enough (more than several k_BT) and Eq. (11) is satisfied.

D. Macroscopic characteristics of the pore

In order to compute the macroscopic characteristics of the pore it is convenient to subdivide the probability density $\varphi^{(n)}(\xi_1)$ into known equilibrium and unknown nonequilibrium parts as it was done in the general theory [13]

$$\tilde{\phi}^{(n)}(\vec{\xi}) \equiv e^{-\tilde{U}_n(\vec{\xi})}\nu^{(n)}(\vec{\xi}), \tag{20}$$

where $\nu^{(n)}$ is related to the local entropy, which is constant in equilibrium conditions [13]. All macroscopic characteristics of the pore could be expressed in terms of ν. Equation (19) could be written as

$$\nu^{(n)}(\vec{\xi}) = \nu^{(n)}(\xi_1) = \begin{cases} \dfrac{\varphi^{(n)}(\xi_1)}{z_n(\xi_1)}, & \vec{\xi} \in \mathfrak{R}^{(n)} \\ 0, & \vec{\xi} \notin \mathfrak{R}^{(n)} \end{cases}. \tag{21}$$

Equation (17) in the steady-state transforms to the following simple equation for ν:

$$\frac{d}{d\xi_1}\left[e^{-U_n^{eff}(\xi_1)}\frac{d\nu^{(n)}(\xi_1)}{d\xi_1}\right] = 0. \tag{22}$$

The boundary conditions of the Eq. (22) are obtained from Eq. (1) using relation (20),

$$\nu^{(n)}(0) = r_1\nu^{(n-1)}(0)$$

$$\nu^{(n)}(l_n) = r_2\nu^{(n-1)}(l_{n-1}), \tag{23}$$

where $r_{1,2} \equiv c_{1,2}e^{U_0(\mp L)}$, l_n is the length of the groove axis in the case of n ions in the pore.

Equation (22) is one-dimensional for any number of ions in the pore and could be solved analytically

$$\nu^{(n)}(\xi_1) = \nu^{(n)}(0) + [\nu^{(n)}(l_n) - \nu^{(n)} \times (0)]\int_0^{\xi_1} e^{U_n^{eff}(\xi')}d\xi' \Big/ \int_0^{l_n} e^{U_n^{eff}(\xi')}d\xi'.$$

Thus, we obtained *analytical* solutions for all occupancy states of the pore. The only quantities, which should be computed numerically are the effective potentials $U_n^{eff}(\xi_1)$.

The probabilities of occupancy states are obtained in the general theory developed in [13] as

$$w_n = \frac{\dfrac{p^{(n)}}{n!}}{\displaystyle\sum_{m=0}^{n_{\max}} \frac{p^{(m)}}{m!}}, \tag{24}$$

where $p^{(n)} = \int_{-L}^{L} dx_1, \ldots, \int_{-L}^{L} dx_n \phi^{(n)}(x_1, \ldots, x_n, t)$ is the norm of $\phi^{(n)}(x_{i_1}, \ldots, x_{i_n}, t)$.

Using Eqs. (24) and (21) the probabilities of occupancy states of the pore could be written as

$$w_n = \frac{\dfrac{q^{(n)}}{M}}{\displaystyle\sum_{i=0} q^{(n)}}, \tag{25}$$

where $q^{(n)} = \int_0^{l_n} d\xi_1 z_n(\xi_1)\nu^{(n)}(\xi_1)$.

The charge density along the pore could be obtained using Eq. (22) from work [13] and Eq. (21)

$$\rho^{(n)}(z) = \frac{1}{q^{(n)}} \sum_{i=1}^{n} \left\{ \int_{-L}^{L} dx_1, \ldots, \int_{-L}^{L} \times dx_{i-1} \int_{-L}^{L} dx_{i+1}, \ldots, \int_{-L}^{L} dx_n e^{-U_n(x_1,\ldots,x_{i-1},z,x_{i+1},\ldots,x_n)} \times \{\nu^{(n)}[\xi_1(x_1,\ldots,x_{i-1},z,x_{i+1},\ldots,x_n)]\} \right\} \quad (26)$$

Finally, the current through the pore in the occupancy state n is obtained using Eq. (18) and Eq. (25) from [13], which defines the current through the given cross section of the channel in given occupancy state

$$J^{(n)}(\xi_1) = -n \frac{D}{q^{(n)}} e^{-U_n^{eff}(\xi_1)} \frac{\partial \nu^{(n)}(\xi_1)}{\partial \xi_1}. \quad (27)$$

The stationary current is obviously independent on ξ_1, thus any value of ξ_1 can be used. The total current through the pore is

$$J = \sum_{i=1}^{M} w_n J^{(n)}(\xi_1)|_{\xi_1=0}. \quad (28)$$

The stationary current can also be expressed in the integral form by rewriting Eq. (27) using the boundary conditions [Eq. (1)] and Eq. (20)

$$J^{(n)} = -n \frac{D}{q^{(n)}} [c_1 \tilde{\phi}^{(n-1)}(x_2', \ldots, x_n') e^{U_n^{eff}(0)} - c_2 \tilde{\phi}^{(n-1)} \times (x_1'', \ldots, x_{n-1}'') e^{U_n^{eff}(l_n)}] / \int_0^{l_n} e^{U_n^{eff}(\xi_1)} d\xi_1. \quad (29)$$

E. Numerical solution

The groove axis is found numerically using Eq. (5) in conjunction with constrained energy minimization, which suppresses possible inaccuracies in finding the bottom of the groove. The number of discrete points, which represent the groove axis depends on the pore occupancy and ranges from 200 to 1000. Additional tests show that this number is enough to obtain all quantities with reasonable accuracy (not shown). Once the groove axis is found, the orthonormal perpendicular vectors [Eq. (9)] are computed in each discrete point by projecting the orts of laboratory coordinate system to the corresponding hyperplane $\mathbb{N}$ and applying standard orthogonalization procedure. The discrete rectangular grid is then defined in the hyperplane $\mathbb{N}$ and z_n is computed by direct multi-dimensional integration according to Eq. (16). The limits of integration are adjusted empirically. Once z_n are known in each discrete point of the groove axis the computations of ν_n and the macroscopic properties of the pore are trivial. This algorithm is implemented in the custom program written in FORTRAN 90.

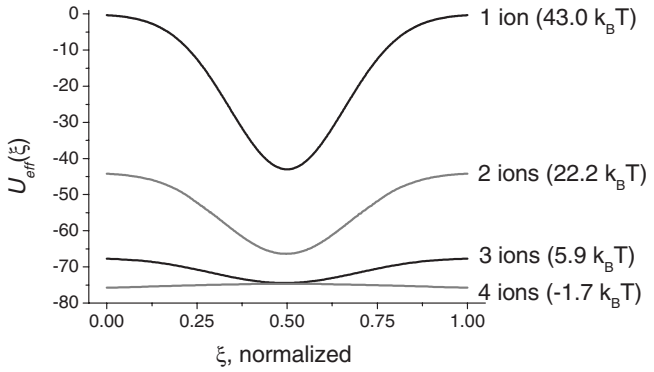

FIG. 3. Effective potentials for various channel occupancies for $A=43$ k$_B$T, $d=3$ Å. The depths of the potentials are shown in parentheses (negative depth corresponds to the energy barrier). The parameters are the same as in Fig. 1.

III. RESULTS

A. Groove axis in different occupancy states

Figure 2(a) shows the grooves in the potentials U_n for of $n=1,\ldots,4$. It is clearly seen that the positions of the ions change in a concerted way along the groove axis. Figures 2(b) and 2(c) visualize the groove axis in two- and three-dimensional space. It is visible that the axis connects the input and the output facets and is surrounded by the "onion shells" of the isolines of U_n.

B. Effective potentials

Figure 3 shows the effective potential U_n^{eff} for $n=1,\ldots,4$. The depth of the effective potential reduces with the increase of n and reaches approximately 6 k_BT for the last stable configuration of ions ($n=3$ for given parameters). The configuration with four ions is already unstable and introduces a small energy barrier to the effective potential. This dependence is universal and observed for all tested values of parameters (not shown), however the last stable occupancy changes with the change of the well depth A and the shielding constant d.

Dramatic decrease of the depth of effective potentials in comparison with U_0 clearly shows the physical reason of the multiple pore occupancy. Indeed, the collective super-ions, which move in the very shallow effective potential, facilitate much larger current though the channel than individual ions, which move in the single-ion potential U_0.

C. Comparison with the generic computational procedure

The approximation of the super-ions itself and the general analytical theory built in [13] are robust and correct. However, the generic computational procedure (referred as GCP hereafter), which was developed in [13], is rather inaccurate. The GCP is completely unspecific and handles arbitrary single-ion energy profiles, but this universality comes at price of high computational intensity and reduced accuracy. In brief, there are three factors, which limit the accuracy of the GCP,

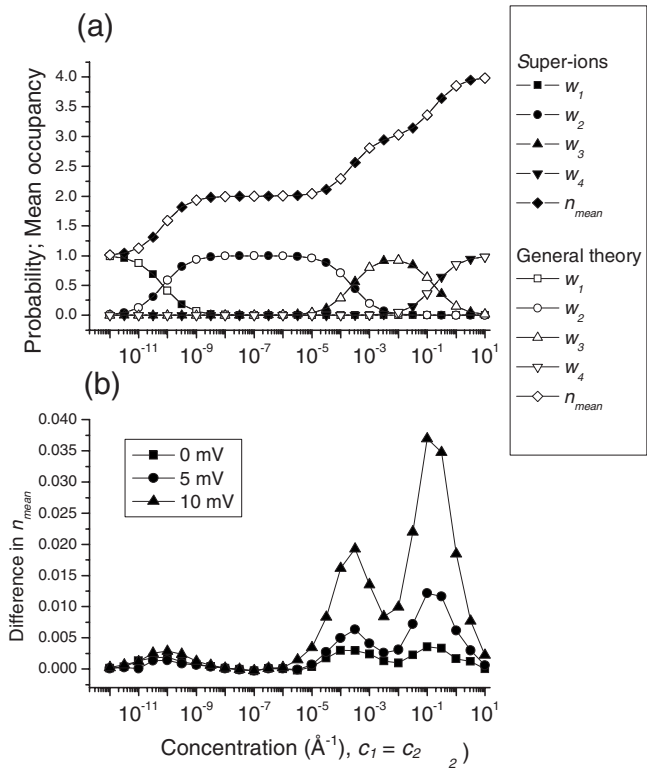

FIG. 4. (a) Concentration dependencies of the mean occupancy n_{mean} and the occupancy probabilities w_n in the approximation of the super-ions and in general theory for $\psi=0$ mV. The parameters are the same as in Fig. 2. (b) The difference in n_{mean} computed in the GCP and in the approximation of the super-ions for various values of ψ.

(1) The single-ion energy profile U_0 has zero derivatives at the ends of the channel, while the majority of potentials, which are commonly used in testing and validation of numerical algorithms, have growing derivative at the boundaries ("boxed" potentials). As a result the precision of the common numerical schemes becomes questionable in our case.

(2) As it is explained in [13] the optimization problem have to be solved instead of the corresponding boundary value problem in order to avoid computation of the fast-growing derivatives of V. We have shown, however, that redundant solutions of this optimization problem exist within machine precision, which leads to unpredictable inaccuracy.

(3) The hierarchical nature of the equations leads to rapid amplification of the errors for each subsequent channel occupancy.

The numerical solution in GCP is correct in equilibrium however the inaccuracy increases with the increase of non-equilibrium factors, such as ψ or the difference of concentrations. The integral characteristics, such as w_n, are expected to be quite accurate near the equilibrium, while the currents $J^{(n)}$ should only be treated qualitatively.

Thus the approximation of the super-ions can be validated against the GCP using the integral characteristics, such as w_n, near the equilibrium. Figure 4(a) shows the concentration dependencies of the channel occupancies w_n and the mean number of ions in the channel in equilibrium. The curves for small membrane potentials (up to $\psi=10$ mV) are visually indistinguishable from equilibrium ones and thus not shown for clarity.

Figure 4(b) shows the difference in the mean number of ions computed in the GCP and in the approximation of the super-ions. There is almost ideal correspondence between the concentration dependencies in equilibrium. This is remarkable taking into account completely different methods of calculations, different underlying approximations and different numerical inaccuracies in our approximation and in GCP. This convinces us that the approximation of the super-ions is very precise in terms of occupancy probabilities in the studied range of parameters. The results of the GCP and our approximation diverge consistently with the increase of membrane potential, but the difference remains very small (less then 1.5%) up to $\psi=10$ mV. Maximal deviations are observed in the transition regions between different occupancy states. The magnitudes of these deviations increase with the increase of occupancy. This behavior is most likely a consequence of the "amplification of errors" in the GCP, which was mentioned above. The comparison for larger values of ψ is not justified due to uncontrollable numerical errors in GCP.

D. Current-voltage relationships

Figure 5(a) shows the current-voltage relationships for different concentrations in the approximation of the super-ions computed using Eq. (29). The curves are rather complex and consist of two distinct parts. The current increases exponentially for small voltages, which is clearly seen in log scale in the inset of Fig. 5(a). The parts of the curves, which correspond to large voltages, are linear or slightly saturating. The transition from exponential to linear parts is smooth and shifts toward larger voltages with the decrease of concentration. The curves for different concentrations eventually converge for the very large voltages.

The shape of the current-voltage relationships reflects complex interplay between the contributions of different occupancy states. This can be illustrated by comparing the current-voltage relationships [Fig. 5(a)] with the dependencies of w_n and the mean occupancy on the voltage (Fig. 5(b)). The mean occupancy increases monotonously with the increase of voltage due to increasing driving force, which "pumps" the ions into the pore. Double occupancy dominates in equilibrium ($\psi=0$) for chosen parameters. The probability of double occupancy w_2 decreases with voltage, while the probability of triple occupancy w_3 increases. The state with four ions (w_4) substitutes the triple occupancy state with the further increase of voltage. This sequential substitution of the dominant occupancy states corresponds to the exponential part of the current-voltage relationship. When the dominant occupancy reaches the maximal number of ions (four in our case), the transition to linear part begins. In the linear regime the pore is saturated with the ions completely, so the current becomes almost independent on concentrations (it depends on the diffusion coefficient D only). As a consequence all curves in Fig. 5(a) converge for very large voltages.

IV. DISCUSSION

The single-file diffusion of several ions in the narrow pores inevitably leads to their concerted motion caused by

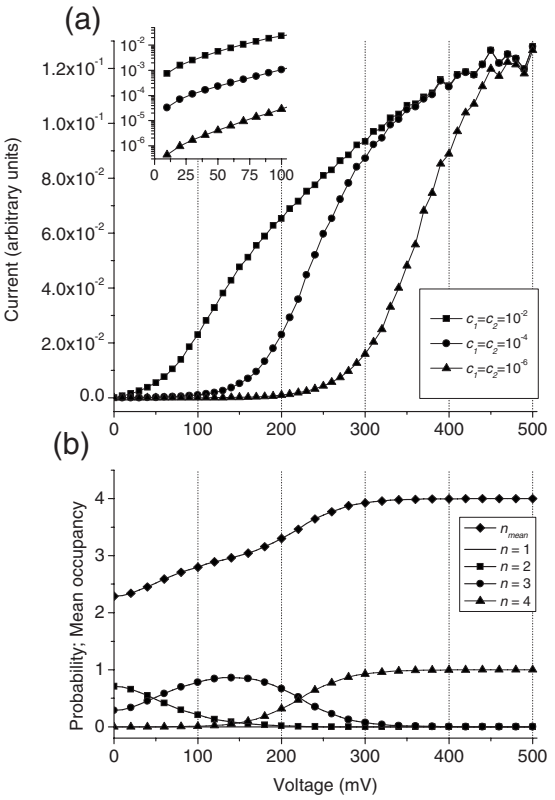

FIG. 5. (a) Current-voltage relationships for indicated values of concentrations (in $Å^{-1}$ units) in the approximation of the super-ions. Inset shows the region of small voltages in log scale to emphasize the exponential shape of the curves. (b) Voltage dependencies of the mean occupancy n_{mean} and occupancy probabilities w_n for $c_1=c_2=10^{-4}$ $Å^{-1}$ [corresponds to middle curve in (a)]. The parameters are the same as in Fig. 2.

the geometrical confinement and the interplay between the single-ion energy profile and the ion-ion interactions, which keeps the ions at certain preferable distances from each other. This corresponds to the existence of well-defined one-dimensional preferable path in the configurational space, which facilitates the conduction. Particularly, similar picture of conductance was postulated on the qualitative level for the KcsA ion channel [2,3,19]. However, there was no consistent theory of such concerted diffusion of multiple ions in the narrow pores.

In our previous work [15] we proposed rather naive theory of concerted single-file motion of ions in the pore, which first introduced the concept of the super-ion. In [15] the super-ion was located at the center of masses of all ions in the pore and was moving in the effective potential composed from U_0 and the averaged ion-ion interactions. Such description relied on multiple assumptions and resulted in a system of quite complex differential equations. In this work we propose another approach to the same problem, which is much more robust and based on the recently developed general theory of the multiparticle diffusion in narrow pores [13]. The introduction of the super-ion in the current work is based on the specific shape of the potential U_n, which possesses a well-defined deep groove corresponding to the most preferable path (in terms of free energy) of multiple ions through the channel. If such groove exists, then the adiabatic approximation could be applied and the multidimensional distribution function of n real ions reduces to one-dimensional distribution function of single quasiparticle (the super-ion). Such reduction could be done for any n (providing that the grooves exist for all occupancies up to n), which dramatically simplifies the problem and allows to avoid complex multidimensional equations. The existence of the deep groove is the only additional assumption in comparison to general theory, which makes our approximation clear and easily controllable. The motion of the super-ions for different occupancy is described by the system of one-dimensional Fokker-Planck equations, which are coupled by simple hierarchical boundary conditions [Eq. (23)]. There are no complex coupling terms, which were present in the work [15] and no additional empirical constants.

Since the concept of the super-ions is an approximation, it is important to validate it against the general theory. The multidimensional equations of the general theory are currently solved numerically by means of generic computational procedure, which produces semiquantitative results. Due to these numerical issues the comparison is currently limited to integral properties, such as the probabilities of occupancy states, and to small deviations from equilibrium. The comparison of occupancy probabilities in equilibrium and for small membrane potentials provide robust test case for our approximation. It is shown that the approximation of the super-ions reproduces the occupancy states w_n extremely well. This means that the probability of finding the system outside the groove is indeed negligible (w_n depend on the norms of the multidimensional distributions $\phi^{(n)}$, which are only computed inside the groove). Thus, all consequent computations, which based on this key approximation, are sufficiently precise.

The approximation of the super-ions can also be a practical way of computing the current and other macroscopic properties of the channel, which are very hard to obtain accurately using the generic computational procedure. The accuracy of the method developed in this work is limited by the approximation of the super-ions itself. In contrast to generic computational procedure the computations are very accurate and very cheap within this approximation. This makes our technique preferable for all potential where the well-defined groove exists.

The approximation of the super-ions is currently targeted on fundamental understanding of the multiion diffusion in the narrow pores. It provides theoretical description of the well-known mechanism of so called "barrier-less knock-on conductance" [2,18]. Indeed, it is shown that the depths of effective potentials for the super-ions become smaller with the increase of occupancy. The potential for the highest stable occupancy is always almost "flat" even if the depth of initial single-ion potential is 50–100 k_BT (Fig. 3). Thus the corresponding super-ion moves almost freely inside the groove and facilitates the "barrier-less conductance," which is a universal feature of the pores with multiple occupancy possessing the smooth bell-like single-ion energy profiles [18].

V. CONCLUSION

The general theory of the single-file multiparticle diffusion in narrow pores developed in [13] can be greatly simplified in rather wide class of specific shapes of the single-ion energy profiles. In such potentials the ions move in highly concerted manner, which corresponds to the existence of narrow and deep groove in the energetic landscape. The motion of multiple ions can be reduced to the motion of single quasiparticle (the super-ion), which moves in one-dimensional effective potential along the groove. It is shown that effective potentials of the super-ions, which correspond to the conducting occupancies of the channel, are essentially flat. This explains the phenomenon of the barrier-less conduction in the narrow channels with multiple occupancy in very elegant way. The approximation of the super-ions also reduces the computational complexity of the problem dramatically in comparison with the generic computational procedure.

ACKNOWLEDGMENT

This work was partially supported by STCU Grant No. 4930.

[1] D. A. Doyle *et al.*, Science **280**, 69 (1998).
[2] S. Berneche and B. Roux, Nature (London) **414**, 73 (2001).
[3] B. Hille, *Ion Channels of Excitable Membranes* (Sinauer Associates Inc., 2001).
[4] G. Hummer, J. C. Rasaiah, and J. P. Noworyta, Nature (London) **414**, 188 (2001).
[5] F. Zhu and K. Schulten, Biophys. J. **85**, 236 (2003).
[6] D. J. Mann and M. D. Halls, Phys. Rev. Lett. **90**, 195503 (2003).
[7] S. Berneche and B. Roux, Biophys. J. **78**, 2900 (2000).
[8] S.-H. Chung, T. W. Allen, and S. Kuyucak, Biophys. J. **82**, 628 (2002).
[9] M. Compoint *et al.*, Biochim. Biophys. Acta **1661**, 26 (2004).
[10] S. Chang *et al.*, Biophys. J. **77**, 2517 (1999).
[11] B. Corry, S. Kuyucak, and S.-H. Chung, Biophys. J. **78**, 2364 (2000).
[12] A. Aksimentiev and K. Schulten, Biophys. J. **88**, 3745 (2005).
[13] V. N. Kharkyanen and S. O. Yesylevskyy, Phys. Rev. E **80**, 031118 (2009).
[14] R. J. Mashl *et al.*, Biophys. J. **81**, 2473 (2001).
[15] S. O. Yesylevskyy and V. N. Kharkyanen, Phys. Chem. Chem. Phys. **6**, 3111 (2004).
[16] P. McGill and M. F. Schumaker, Biophys. J. **71**, 1723 (1996).
[17] W. Stephan, B. Kleutsch, and E. Frehland, J. Theor. Biol. **105**, 287 (1983).
[18] S. O. Yesylevskyy and V. N. Kharkyanen, Chem. Phys. **312**, 127 (2005).
[19] B. Hille and W. Schwarz, J. Gen. Physiol. **72**, 409 (1978).